

Band structure effects in time-dependent electron transport through the quantum dot

T. Kwapiński, R. Taranko,* and E. Taranko

Institute of Physics, M. Curie-Skłodowska University, 20-031 Lublin, Poland

(Received 13 August 2001; revised manuscript received 6 February 2002; published 17 July 2002)

The evolution operator method is used to study the electron tunneling through the quantum dot. The external microwaves fields are applied to both the dot and leads. Under the adiabatic approximation, the formulas for the time-dependent quantum dot charge and current flowing through the quantum dot are obtained. The time-averaged quantum dot charge, tunneling current, and derivatives of the time-averaged tunneling current with respect to the source drain and gate voltages are calculated beyond the wide band limit for the two-dimensional tight-binding spectrum of the leads electrons. The influence of the singularities of the lead density of states on the photon-assisted tunneling peaks is also discussed.

DOI: 10.1103/PhysRevB.66.035315

PACS number(s): 73.40.Gk, 73.23.-b, 73.50.-h

Electron transport in mesoscopic devices has been intensively studied recently. Especially interesting are the transport properties of the quantum dot (QD) under the influence of external time-dependent fields. The QD was investigated for various configurations of time-dependent parameters. New effects have been observed, e.g., photon-electron pump, side band effect, electron turnstile, and others (e.g., Ref. 1). The experiments in which the heights of barrier are modulated are now available and the turnstile effect has been observed (e.g., Ref. 2). Other works have addressed the response of the QD to an ac bias applied between two leads or applied simultaneously between two leads and to a QD (time-dependent gate voltage), see, e.g., Ref. 3.

In the simplest case the Hamiltonian of the QD with multiple energy levels (without the electron-electron Coulomb interaction) coupled to two leads (right and left) in the presence of external microwave (MW) fields which are applied to both the dot and leads, can be written as $H = H_1 + V$, where

$$H_1 = \sum_{\vec{k}_\alpha} \epsilon_{\vec{k}_\alpha}^-(t) a_{\vec{k}_\alpha}^- a_{\vec{k}_\alpha}^{+\dagger} + \sum_n \epsilon_n(t) a_n^+ a_n, \quad (1)$$

$$V = \sum_{\vec{k}_\alpha, n} V_{\vec{k}_\alpha, n} a_{\vec{k}_\alpha}^- a_n^+ + \text{H.c.}, \quad (2)$$

where $\alpha = R, L$ denotes the right (R) or left (L) lead in the system. The operators $a_{\vec{k}_\alpha}^- (a_{\vec{k}_\alpha}^{+\dagger})$, $a_n (a_n^+)$ denote annihilation (creation) operators for conduction electrons with the wave vector \vec{k} in the lead α and for electrons in the n th energy level of the QD, described by the functions $|\vec{k}_\alpha\rangle$ and $|n\rangle$, respectively. The hybridization matrix element between the conduction electron with energy $\epsilon_{\vec{k}_\alpha}^-$ in the lead α and the localized electron on the n th energy level of the QD is denoted by $V_{\vec{k}_\alpha, n}$ and $\epsilon_n(t)$ is the single particle energy of an electron on the n th energy level of the QD.

Under the adiabatic approximation the single-electron energies of the time-dependent driven system, Eqs. (1), (2), can be represented in the form $\epsilon_{\vec{k}_\alpha}^-(t) = \epsilon_{\vec{k}_\alpha}^- + \Delta_\alpha \cos \omega t$, $\epsilon_n(t) = \epsilon_n + \Delta_n \cos \omega t$, i.e., the energy levels of the leads and QD are driven by the MW fields with frequency ω and ampli-

tudes Δ_α and Δ_n , respectively. Without describing the formalism, which has already been discussed in detail (see, e.g., Ref. 3), we recall that the general formula for the current flowing, e.g., from the left lead into the QD is usually expressed in terms of the QD retarded Green function $G^r(t, t_1)$. However, $G^r(t, t_1)$ satisfies the Dyson equation with subsequent double time integrations and for the time-dependent Hamiltonian it is a very difficult task to calculate it. For that reason in literature, as a rule, the wide band limit (WBL) is used for calculations of the corresponding self-energy $\Sigma^r(t, t_1)$. In this approximation $\Sigma^r(t, t_1)$ is proportional to $\delta(t - t_1)$ and, in consequence, $G^r(t, t_1)$ can be obtained in a closed, simple form. WBL has been widely used in calculations of the time-independent, as well as the time-dependent properties of mesoscopic systems (e.g., Refs. 2, 3). This approximation is justified under the condition that the density of states of the leads varies slowly with energy over a range of several Γ around the QD resonant level, Γ being the linewidth of the QD energy level. In addition, the QD resonant level should be localized not close to the edges or top of the energy bands of the leads. In practice, however, a situation can occur when this condition is not satisfied. One should remember, that the density of states for some two-dimensional electron systems possesses a singular structure at the band center. Therefore, the experimental conditions imposed on some mesoscopic devices may lead to the situation in which the QD resonance level will be localized near the singular points of the lead energy band structure or near the energy band edges. So the band structure and, in particular, van Hove singularities in the leads can influence the tunneling current across the QD. Such studies have been carried out for the QD placed between the leads to which a constant bias $\mu_L - \mu_R$, $\mu_L (\mu_R)$ being the chemical potential of the left (right) lead, was applied.⁴ The singular structure due to the singularities of the lead density of states was observed in the QD density of states and in the nonlinear conductance voltage curves.

In this paper we are going to study the influence of the singularities of the leads band structure on the QD charge and electron transport through the QD in the case when the MW external fields are applied to this system. Therefore we are forced to go beyond WBL and within the formalism of the nonequilibrium Green functions it is extremely difficult

to calculate, e.g., the time-dependent current $j_L(t)$ tunneling from the left-hand lead to the QD or the QD charge. Therefore, in the following, we calculate the QD charge and current flowing in the system using the evolution operator method. This method was successfully used, e.g., in the problems of the time-dependent ionization of atoms scattered on metal surfaces.⁵

The paper is arranged as follows. First we give the formulas for time-dependent current and QD charge for the QD connected to leads characterized by some electron band structure. Next, the time-dependent QD charge and the current flowing through the system vs the gate voltage and the source-drain voltage are studied assuming the two-dimensional tight-binding spectrum for leads electrons. We consider that in the half-filled lead electron energy bands in this case the influence of the density of states singularities should be important. We also consider the influence of the lead band structure singularities on the photon-assisted tunneling (PAT) peaks. Finally, we study the influence of the energy band edges on the average current flowing in the system.

The dynamical evolution of a QD coupled to two leads can be described in terms of the time-evolution operator $U(t, t_0)$ (in the interaction representation) given by the equation of motion (e.g., Ref. 5):

$$i \frac{\partial}{\partial t} U(t, t_0) = \tilde{V}(t) U(t, t_0), \quad (3)$$

where

$$\begin{aligned} \tilde{V}(t) &= U_0(t, t_0) V(t) U_0^\dagger(t, t_0), \\ U_0(t, t_0) &= \exp\left(i \int_{t_0}^t dt' H_1(t')\right). \end{aligned} \quad (4)$$

Here we assume that the interaction between the QD and leads is switched on in the distant past t_0 , i.e., the hybridization matrix elements equal to zero for $t \leq t_0$ and take the constant values for $t > t_0$. The knowledge of the matrix elements of $U(t, t_0)$ is sufficient to calculate both the charge localized on the QD and the electric current flowing through the system under consideration.

The total QD charge is given as follows (see Ref. 5):

$$\begin{aligned} n(t) &= \sum_i n_i(t) = \sum_i \left(\sum_j n_j(t_0) |U_{ij}(t, t_0)|^2 \right. \\ &\quad \left. + \sum_{\vec{k}_\alpha} n_{\vec{k}_\alpha}(t_0) |U_{i, \vec{k}_\alpha}(t, t_0)|^2 \right), \quad i, j = 1, \dots, m, \end{aligned} \quad (5)$$

where m denotes the number of the QD energy levels. Here $U_{ij}(t, t_0)$ and $U_{i, \vec{k}_\alpha}(t, t_0)$ denote the matrix elements of $U(t, t_0)$ calculated within the basis functions containing the single-particle functions $|\vec{k}_L\rangle$, $|\vec{k}_R\rangle$, and $|i\rangle$. $n_j(t_0)$ and $n_{\vec{k}_\alpha}(t_0)$ represent the initial filling of the corresponding single-particle states. The tunneling current, e.g., from the

left lead into the QD, can be calculated from the evolution of the total number of electrons in the left lead $n_L(t)$ (see Ref. 3): $j_L(t) = -e(d/dt)n_L(t)$, where

$$\begin{aligned} n_L(t) &= \sum_{\vec{k}_L} \left(\sum_j n_j(t_0) |U_{\vec{k}_L, j}(t, t_0)|^2 \right. \\ &\quad \left. + \sum_{q_L} n_{q_L}(t_0) |U_{\vec{k}_L, q_L}(t, t_0)|^2 \right. \\ &\quad \left. + \sum_{\vec{k}_R} n_{\vec{k}_R}(t_0) |U_{\vec{k}_L, \vec{k}_R}(t, t_0)|^2 \right). \end{aligned} \quad (6)$$

In the following we need only to know the matrix elements of the evolution operator $U(t, t_0)$ present in expressions for $n(t)$ and $n_L(t)$. For example, the integrodifferential equations for the matrix elements $U_{ij}(t, t_0)$ and $U_{j, \vec{k}_\alpha}(t, t_0)$ needed in calculations of the QD charge $n(t)$ can be obtained using Eqs. (3), (4) and are as follows:

$$\begin{aligned} \frac{\partial}{\partial t} U_{ij}(t, t_0) &= - \sum_l \int_{t_0}^t dt' \mathcal{K}^{il}(t, t') U_{lj}(t', t_0), \\ i, j, l &= 1, \dots, m, \end{aligned} \quad (7)$$

$$\begin{aligned} \frac{\partial}{\partial t} U_{j, \vec{k}_\alpha}(t, t_0) &= -i \tilde{V}_{j, \vec{k}_\alpha}(t) \\ &\quad - \sum_l \int_{t_0}^t dt' \mathcal{K}^{jl}(t, t') U_{l, \vec{k}_\alpha}(t', t_0), \end{aligned} \quad (8)$$

where

$$\mathcal{K}^{il}(t, t') = \sum_{\vec{k}_\alpha} \tilde{V}_{i, \vec{k}_\alpha}(t) \tilde{V}_{\vec{k}_\alpha, l}(t') \equiv \mathcal{K}_L^{il}(t, t') + \mathcal{K}_R^{il}(t, t'). \quad (9)$$

In order to calculate the tunneling current $j_L(t)$ we have to obtain, in the first step, $n_L(t)$ and after lengthy algebraic manipulations the result in formula for $j_L(t)$ is as follows:

$$\begin{aligned} j_L(t) &= - \sum_j n_j(t_0) \sum_{l_1, l_2} \Psi(l_1, l_2, j; t_0, t) \\ &\quad + 2 \operatorname{Im} \sum_{\vec{k}_L} n_{\vec{k}_L}(t_0) \sum_{l_1} \tilde{V}_{l_1, \vec{k}_L}(t) U_{l_1, \vec{k}_L}^*(t, t_0) \\ &\quad + \sum_{q_\alpha} n_{q_\alpha}(t_0) \sum_{l_1, l_2} \Psi(l_1, l_2, q_\alpha; t_0, t), \end{aligned} \quad (10)$$

where

$$\begin{aligned} \Psi(a, b, c; t_0, t) &= \int_{t_0}^t dt' \mathcal{K}_L^{ba}(t, t') U_{bc}^*(t, t_0) U_{ac}(t', t_0) \\ &\quad + \int_{t_0}^t dt' \mathcal{K}_L^{ba}(t', t) U_{bc}^*(t', t_0) U_{ac}(t, t_0). \end{aligned} \quad (11)$$

The formulas for the QD charge and for the current tunneling between the left lead and the QD, Eqs. (5), (10), together with the equations for required matrix elements of the evolution operator, Eqs. (7)–(9), are the central results of this paper. In order to use them in numerical calculations we have to specify only the form of the matrix elements of $\tilde{V}(t)$ and calculate $\mathcal{K}_L^{il}(t, t')$ and $\mathcal{K}_R^{il}(t, t')$. We have

$$\tilde{V}_{j\bar{k}_\alpha}(t) = V_{j\bar{k}_\alpha} \exp[-i(\Delta_j - \Delta_\alpha)\sin(\omega t)/\omega - i(\epsilon_j - \epsilon_{\bar{k}_\alpha})t], \quad (12)$$

$$\mathcal{K}_\alpha^{l_1, l_2}(t, t') = V_{l_1, \alpha} V_{\alpha, l_2} \mathcal{D}_\alpha(t - t') \exp[i(\epsilon_{l_1} t - \epsilon_{l_2} t') + i(\Delta_{l_1} - \Delta_\alpha)\sin(\omega t)/\omega - i(\Delta_{l_2} - \Delta_\alpha)\sin(\omega t')/\omega], \quad (13)$$

where $\mathcal{D}_\alpha(t - t')$ is the Fourier transform of the density of states of the α th lead and we have assumed that the matrix elements $V_{\bar{k}_\alpha, n} \equiv V_{\alpha, n}$ are \bar{k} independent.

We assume the temperature $T=0$ K and the time-averaged current $\langle j(t) \rangle$ is obtained by averaging $j(t)$ over the period $2\pi/\omega$. The similar procedure is applied to the calculation of the QD average charge. Without loss of generality we assume that the energy band of the right lead is localized in the energy range $(-W_R/2, W_R/2)$, W_R being the bandwidth, and take $W_L = W_R = W$. We take the chemical potential of the right lead μ_R as the energy measurement reference point $\mu_R = 0$. The potential drop between the left and right leads is given by $\mu_L - \mu_R = eV_{s-d}$ and V_{s-d} is the measured voltage between source and drain. In experiments the gate voltage controls the position of QD's energy level ϵ_d and to mimic measurements of the QD charge or current vs gate voltage we have calculated them against ϵ_d . To study the effect of the leads band structure on the electron transport through the QD, we have assumed the two-dimensional tight binding (2D-TB) simple cubic crystal spectrum for leads conduction electrons, which is known to possess the logarithmic singularity in the middle of the band. Before we start to analyze the results, let us discuss the relation between the measured experimental linewidth parameter $\Gamma = (\Gamma_L + \Gamma_R)/2$ (we assume symmetrical barriers) and $V_{\bar{k}_\alpha, j}$ entering the theory. Considering the one-level QD we use the abbreviated form for the hybridization matrix elements $V_{\bar{k}_\alpha, j}$ simply as $V_{\bar{k}_\alpha}$. In the WBL the effective linewidth Γ_α is defined as follows: $\Gamma_\alpha = 2\pi \sum_{\bar{k}_\alpha} |V_{\bar{k}_\alpha}|^2 \delta(E - \epsilon_{\bar{k}_\alpha})$, and the values of $V_{\bar{k}_\alpha}$ does not enter the final expressions for the current or QD charge. Contrary to this case, $V_{\bar{k}_\alpha}$ enters explicitly into our expressions for $j_L(t)$ and $n(t)$. In this paper we have estimated $V_{\bar{k}_\alpha}$ (assuming its \bar{k} independence, $V_{\bar{k}_\alpha} = V_\alpha$) using the relation $\Gamma_\alpha = 2\pi |V_\alpha|^2 / W_\alpha$. For calculations we assumed $W_\alpha = 100\Gamma_\alpha$ and take $\hbar = e = 1$ units and all the energies are in units of Γ_R unless otherwise specified in this paper.

In Fig. 1 in the left panels we show the time-averaged QD charge, tunneling current and the derivative of the tunneling current with respect to the QD energy level ϵ_d . In the right panels the corresponding differences ($\Delta\langle n(t) \rangle$, $\Delta\langle j_L(t) \rangle$,

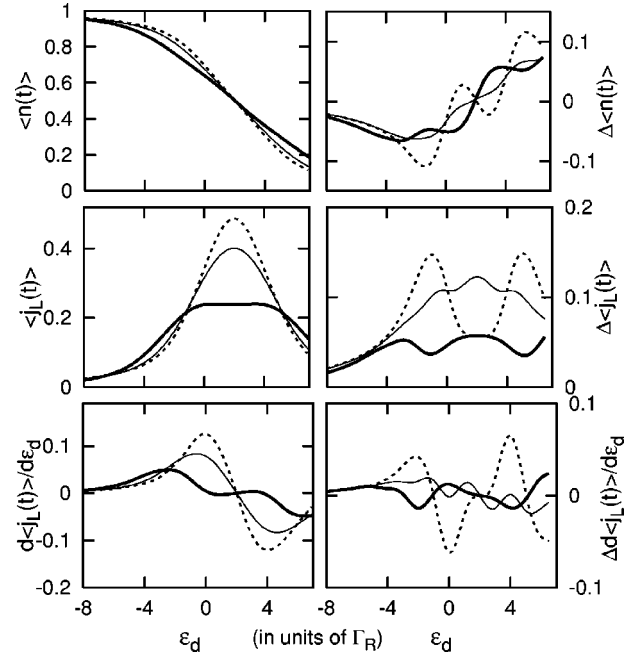


FIG. 1. The time averaged QD charge $\langle n(t) \rangle$, tunneling current $\langle j_L(t) \rangle$, and derivative $d\langle j_L(t) \rangle/d\epsilon_d$ (in arb. units) vs ϵ_d obtained for 2D-TB leads DOS (left panels). In the right panels the corresponding differences between the results shown in the left panels and those obtained within WBL ($\Delta\langle n(t) \rangle$, $\Delta\langle j_L(t) \rangle$, and $\Delta d\langle j_L(t) \rangle/d\epsilon_d$) are given. The thick (thin) curves correspond to $\Delta_L = 8$, $\Delta_L = 4$, $\Delta_R = 0$ ($\Delta_L = 4$, $\Delta_d = 2$, $\Delta_R = 0$), and $\omega = 2$, $\mu_R = 0$, $\mu_L = 4$. The dashed curves correspond to the time-independent case.

and $\Delta d\langle j_L(t) \rangle/d\epsilon_d$) between the results obtained for 2D-TB leads DOS and obtained within WBL are given. The dashed lines correspond to the static case ($\omega = 0$) and the solid lines correspond to the time-dependent transport. One can see, that, e.g., for $\epsilon_d = 1$, the tunneling current calculated for 2D-TB leads DOS is greater than that obtained within WBL up to $\sim 30\%$ while for $\epsilon_d = 1$ up to $\sim 150\%$ for the static case and this difference decreases with increasing amplitude Δ_L ($\Delta_d = \Delta_L/2$, $\Delta_R = 0$). It is interesting that the $\Delta\langle j_L(t) \rangle$ curves for different Δ_L exhibit local minima or maxima at the same ϵ_d . For example, $\Delta\langle j_L(t) \rangle$ for the static case possesses a local minimum for $\epsilon_d = 2$ (the middle point between the chemical potentials μ_L and μ_R) but for the time-dependent case we observe local maxima, greater for $\Delta_L = 4$ and lesser for greater amplitude $\Delta_L = 8$. As for the time averaged QD charge, for positive values of ϵ_d the relative differences $\Delta\langle n(t) \rangle / \langle n(t) \rangle_{\text{WBL}}$ are greater up to $\sim 100\%$ for the static case ($\epsilon_d = 5$) and approximately up to 20% for the dynamical case. However, for negative values of ϵ_d these relative differences are small. Note, that for the time-dependent case for ϵ_d greater (lesser) than the middle point between the leads chemical potentials ($\epsilon_d = 2$) these differences are positive (negative). The bottom panels show the derivative $d\langle j_L(t) \rangle/d\epsilon_d$ vs ϵ_d and the corresponding differences obtained for two considered models of the leads DOS. As before, the greatest differences are observed for the static case (dashed lines) for QD energy levels ϵ_d equal to the chemical potentials μ_L or μ_R . For the time-dependent trans-

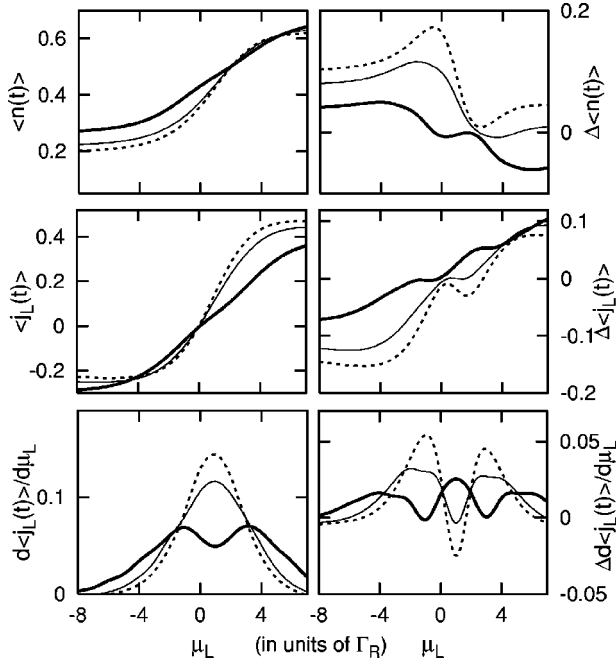


FIG. 2. The time averaged QD charge $\langle n(t) \rangle$, tunneling current $\langle j_L(t) \rangle$, and derivative $d\langle j_L(t) \rangle/d\mu_L$ (in arb. units) vs μ_L obtained for 2D-TB leads DOS (the left panels). In the right panels the corresponding differences between the results showed in the left panels and those obtained within WBL ($\Delta\langle n(t) \rangle$, $\Delta\langle j_L(t) \rangle$, and $d\langle j_L(t) \rangle/d\mu_L$) are given. The thick, thin, and dashed curves correspond to $\Delta_L=8, 4$, and 2, respectively, for $\omega=2$, $\epsilon_d=1$, $\mu_R=0$ and $\Delta_d=\Delta_L/2$, $\Delta_R=0$.

port these differences are much smaller and hardly depend on amplitudes Δ_L and Δ_d , contrary to $\Delta\langle j_L(t) \rangle$ which are greater for smaller values of Δ_L and Δ_d .

In Fig. 2 we give the time averaged values of the QD charge, tunneling current and differential conductance $\langle n(t) \rangle$, $\langle j_L(t) \rangle$, and $d\langle j_L(t) \rangle/d\mu_L \equiv G$, respectively, as functions of the chemical potential μ_L for fixed $\mu_R=0$. The left panels show the results obtained for 2D-TB leads DOS and right panels shows the corresponding differences $\Delta\langle n(t) \rangle$, $\Delta\langle j_L(t) \rangle$, and ΔG vs μ_L of the results obtained for 2D-TB DOS and within WBL approximation. Note, that essentially no differences are observed for the QD charge calculated for two considered leads DOS only for a very special set of parameters $\mu_L=2$ and QD energy level put in the middle between μ_L and μ_R . For other chemical potentials μ_L , the relative differences, $\Delta\langle n(t) \rangle/\langle n(t) \rangle_{\text{WBL}}$, become very large, up to $\sim 120\%$ for smaller amplitudes Δ_L ($\Delta_L=2$) and up to $\sim 20\%$ for greater Δ_L ($\Delta_L=8$). Similar results are also observed for the tunneling current. Now, approximately only at $\mu_L=\mu_R=0$ there are minor differences but for large positive μ_L the relative differences increase up to $\sim 30\%$ irrespective of the amplitude Δ_L and up to ~ 170 , ~ 100 , and $\sim 30\%$ for large negative μ_L and $\Delta_L=2, 4$, and 8, respectively. As for the differential conductance (bottom panels) the WBL produces, generally, much narrower peaks, although their heights are nearly the same for greater amplitudes Δ_L . Only for small amplitudes Δ_L the conductance peak calculated for

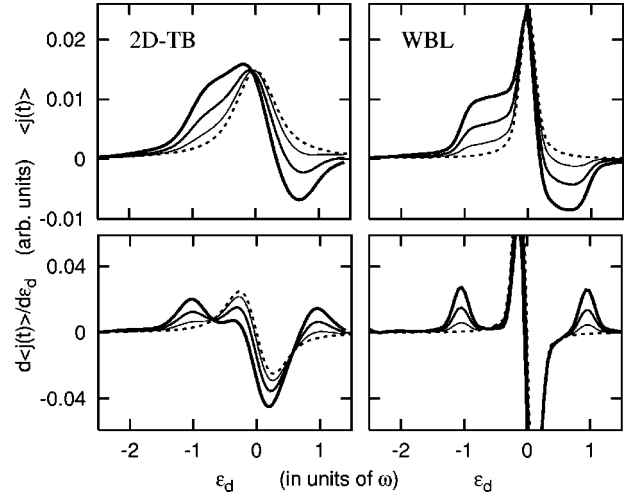


FIG. 3. Left panels: the average current $\langle j_L(t) \rangle$ and derivative $d\langle j_L(t) \rangle/d\epsilon_d$ vs ϵ_d for external field applied only to the right lead in the case of the 2D-TB leads DOS. The solid curves correspond to $\Delta_R/\omega=0.3$ (thin lines), 0.5, and 0.7 (thick lines). The dotted curve is the resonant peak without external field. The parameters are $\Gamma_L=\Gamma_R=0.1\omega$ and $\mu_L=-\mu_R=0.05\omega$. For comparison, on the right panels the same as on the left but obtained within WBL.

2D-TB DOS is lower and simultaneously its halfwidth is twice as much as this one obtained within WBL.

In the next step we consider the influence of the lead DOS structure on the photon-assisted tunneling through a quantum dot. In experiment, in average current vs gate voltage curve, a “shoulder” is observed on the left side of the main resonant peak for the case of a MW field applied on one lead

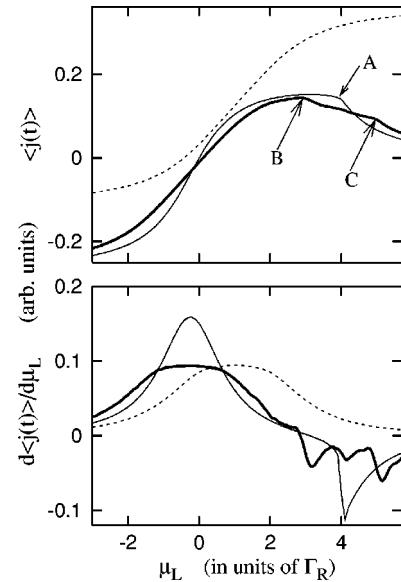


FIG. 4. The average current $\langle j_L(t) \rangle$ and derivative $d\langle j_L(t) \rangle/d\mu_L$ calculated within WBL (dotted lines) and for rectangular leads DOS (solid lines) with μ_L and μ_R lying near the lower band edges. The parameters (in $\Gamma_L=\Gamma_R$ units) are $\mu_R=0$, $\epsilon_d=1$, $\Delta_L=1.5$, and $\omega=1$. The thin (thick) lines correspond to the time-independent (time-dependent) case. The external MW field is applied only to the left lead.

only.¹ In Fig. 3 we compare the structure of the main resonant peak in the average current $\langle j_L(t) \rangle$ and the derivative $d\langle j_L \rangle / d\epsilon_d$ plotted vs ϵ_d obtained within WBL (Ref. 3) (right panels) and calculated for 2D-TB leads DOS (left panels) at half-filled bands. The parameters was taken as in Ref. 2 and the dashed (solid) curves correspond to $\omega=0$ ($\omega \neq 0$). The remarkable differences are visible for negative values of ϵ_d . The main resonant peaks are broader and lower and their height is almost independent on the amplitude Δ_R . For small Δ_R the “shoulders” are almost invisible but with increase of Δ_R , they getting visible and their values getting larger in comparison with WBL results. Nevertheless, in both calculations the indications of the photon-assisted tunneling for $\epsilon_d = \pm 1$ are clearly visible (lower panels of Fig. 3).

In the last step we have considered the case when the lead energy bands are nearly empty, i.e., μ_L and μ_R are located in the vicinity of lower band edges. In such cases the WBL is not applicable. We have performed the calculations for rectangular lead DOS for MW field applied only to the left lead. In Fig. 4 we show $\langle j_L(t) \rangle$ (upper panel) and $d\langle j_L \rangle / d\mu_L$ (lower panel) vs μ_L . The thick (thin) lines correspond to the time-dependent (time-independent) case. For comparison, we also show the time-dependent WBL results (dotted lines), although we remember that for these parameters this approximation is not reliable. Inapplicability of WBL is clearly visible. It should be remarked that there are some interesting points on the current curves. The point A (the time-

independent case) corresponds to the situation when the lower edge of the left lead energy band equals to μ_R . Beginning from that point the current decreases with increasing μ_L . In the time-dependent case the points B and C correspond to such values of μ_L at which the lower edge of the left lead energy band attains [during oscillations of $\epsilon_{k_L}(t)$] approximately value of μ_R . These points are clearly visible on the conductance curves (lower panel of Fig. 4).

In conclusions, we have studied the electron tunneling through the QD in the presence of the time-dependent fields. The one-level QD without Coulomb interaction was considered. By using the evolution operator method the time-dependent and time-averaged QD charge, tunneling current, and derivatives of the time-averaged tunneling currents with respect to the source drain and gate voltages beyond the wide band limit were calculated. To study the effect of the leads electron band structure the two-dimensional tight binding spectrum with logarithmic singularity in the middle of the band was assumed. We found that the differences in the QD charge, tunneling current and differential conductance obtained for 2D-TB leads DOS and for structureless DOS within WBL are relatively large, especially for half-filled leads energy bands and for QD energy levels lying in the vicinity of the van Hove singularities in leads. We also found that the photon-assisted tunneling peaks are lower and broader in comparison with these one obtained for structureless lead density of states.

*Corresponding author. Electronic address: taranko@tytan.umcs.lublin.pl

¹L.P. Kouwenhoven, A.T. Johnson, N.C. van der Vaart, A. van der Enden, C.J.P.M. Harmans, and C.T. Foxon, *Z. Phys. B: Condens. Matter* **85**, 381 (1991); L.P. Kouwenhoven, S. Jauhar, J. Orenstein, P.L. McEuen, Y. Nagamune, J. Motohisa, and H. Sakaki, *Phys. Rev. Lett.* **73**, 3443 (1994);

²Qing-feng Sun and Tsung-han Lin, *Phys. Rev. B* **56**, 3591 (1997)

³Qing-feng Sun and Tsung-han Lin, *J. Phys.: Condens. Matter* **9**,

4875 (1997); Antti-Pekka Jauho, N.S. Wingreen, and Y. Meir, *Phys. Rev. B* **50**, 5528 (1994); R. López, R. Aguado, G. Platero, and C. Tejedor, *Photonics Spectra* **6**, 379 (2000)

⁴M. Krawiec, T. Domański, and K.I. Wysokiński, *Acta Phys. Pol. A* **94**, 411 (1998)

⁵T.B. Grimley, V.C.J. Bhasu, and K.L. Sebastian, *Surf. Sci.* **121**, 305 (1983); M. Tsukada and N. Shima, in *Dynamical Processes and Ordering on Solid Surfaces*, edited by A. Yoshimori and M. Tsukada (Springer Verlag, Berlin, 1995), p. 34.